DALTON
FULL PAPER

Synthesis, magnetic properties, and electronic spectra of mixed ligand bis(β-diketonato)chromium(III) complexes with a chelated nitronyl nitroxide radical: X-ray structure of $[Cr(dpm)_2(NIT2py)]PF_6$ †

Yasunori Tsukahara, Atsushi Iino, Takafumi Yoshida, Takayoshi Suzuki and Sumio Kaizaki *

Department of Chemistry, Graduate School of Science, Osaka University, Toyonaka, Osaka, 560-0043, Japan. E-mail: kaizaki@chem.sci.osaka-u.ac.jp

Received 9th May 2001, Accepted 6th November 2001
First published as an Advance Article on the web 17th December 2001

A new series of nine nitronyl nitroxide Cr(III) complexes with various β-diketonates, $[Cr(\beta\text{-diketonato})_2(NIT2py)]PF_6$, have been synthesized where NIT2py is 2-(2′-(pyridyl)-4,4,5,5-tetramethyl-4,5-dihydro-1*H*-imidazolyl-3-oxide-1-oxyl, and their structures, magnetic and optical properties have been examined. X-Ray analysis of $[Cr(dpm)_2(NIT2py)]PF_6$ (monoclinic, space group $P2_1/a$, $a = 13.960(4)$, $b = 31.19(1)$, $c = 13.940(4)$, $Z = 4$) demonstrated that NIT2py coordinated to Cr(III) as a bidentate six-membered chelate. Variable-temperature magnetic susceptibility measurements indicated the antiferromagnetic interaction between Cr(III) and NIT2py with a variety of the magnetic coupling constant J values for these complexes. From the variable temperature or solvent dependent UV–vis spectra and MCD, and/or the resonance Raman spectra of the bis(β-diketonato)(NIT2py) Cr(III) complexes, the absorption components centered around 13.3×10^3 cm^{-1} were assigned to the formally spin-forbidden d–d transition within the t_{2g} subshell associated with the intensity enhancement and the newly appeared vibronic bands around $(16.0–18.0) \times 10^3$ cm^{-1} were due to the metal–ligand charge transfer [t_{2g}–SOMO(π*) MLCT] transitions. The change of their spectroscopic characteristics with varying the β-diketonato ligands is discussed in connection with the antiferromagnetic coupling constant J values on the basis of the exchange mechanism along with the coligand effect. The luminescence spectra which show a large Stokes shift suggest the antiferromagnetic interaction in the lowest excited states originates from the ^2E or $^2T_1$ level of the Cr(III) moiety.

Introduction

There have been a number of spectroscopic investigations [1–6] on multi-spin exchange coupled systems consisting of paramagnetic metal ions, while metal complexes containing nitroxide radicals such as several derivatives of 4,4,5,5-tetramethyl-4,5-dihydro-1*H*-imidazolyl-3-oxide-1-oxyl (NIT) have been studied from a viewpoint of molecular magnets.[7–10] The first spectroscopic study on paramagnetic metal complexes with the NIT2py radical ligand was our recent report of two series of mixed ligand NIT2py nickel(II) complexes,[11] $[Ni(\beta\text{-diketonato})_2(NIT2py)]$ and $[Ni(\beta\text{-diketonato})(tmen)(NIT2py)]^+$ (tmen = *N,N,N′,N′*-tetramethylethylenediamine) with various types of β-diketonate ligands, followed by a preliminary communication for a limited number of bis(β-diketonato) (NIT2py) complexes of Ni(II) and Cr(III).[12] The NIT2py Ni(II) complexes were found to show a coligand effect (or a substituent effect) of the β-diketonates on the formally spin-forbidden d–d transition intensities or NMR contact shifts in relation to the magnetic exchange coupling constants. Very recently, we reported the magnetic and spectroscopic properties of *cis* (Cl)–*trans* (py)-$[MCl_2(IM2py)_2]$ {M = Mn(II), Co(II), Ni(II) or Zn(II); IM2-py = 2-(2-pyridyl)-4,4,5,5-tetramethylimidazoline-1-oxy}[13] and tetrahedral four-coordinate $[MCl_2(NITmepy)]$ [NITmepy = 4,4,5,5-tetramethyl-2-(6-methyl-2-pyridyl)imidazolin-1-oxide 3-oxyl; M=Co(II), Ni(II), Zn(II)].[14] On the other hand, only one of the corresponding Cr(III) complexes, $[Cr(acac)_2(NIT2py)]ClO_4$,[12] has been prepared and preliminarily characterized by the spectroscopic methods with no X-ray structural evidence for the NIT2py chelation. Further investigation extending to a series of this moderately coupled type of β-diketonato Cr(III) complexes with t_{2g} magnetic orbitals could be invaluable in order to explore expected regulations of the magnetic and optical properties with variation of β-diketonates in comparison with the corresponding Ni(II) complexes with e_g magnetic orbitals. This may be impossible for the strongly coupled types of semiquinone and phenoxy radical Cr(III) complexes, because in this case there has been demonstrated to be large temperature independent intensity enhancement in the spin-forbidden transitions due to strong antiferromagnetic interactions in the ground state.[5]

In this article, the synthesis of a series of NIT2py Cr(III) complexes with various types of β-diketonates and a magnetic and spectroscopic study together with X-ray structural analysis is presented in order to reveal the relation between the optical and magnetic properties in comparison with those of the Ni(II) complexes.

Experimental

Ligand

The radical ligand NIT2py was prepared by the literature method.[15] The β-diketonates were commercially available [β-diketone = Hacac (2,4-pentanedione), Hdbm (1,3-diphenyl-1,3-propanedione), Hbzac (1-phenyl-1,3-butanedione), HacaMe (3-methyl-2,4-pentanedione), HacaEt (3-ethyl-2,4-pentanedione), Haca^{n}Bu (3-*n*-butyl-2,4-pentanedione), HacaPh (3-phenyl-2,4-pentanedione), Hdpm (2,2,6,6-tetramethyl-3,5-heptanedione), HMehp (6-methyl-2,4-heptanedione].

† Electronic supplementary information (ESI) available: variable temperature magnetic susceptibilities with each fitting for the two spin systems and UV-vis spectra for complexes **2**–**9**. See http://www.rsc.org/suppdata/dt/b1/b104092h/

DOI: 10.1039/b104092h

Syntheses of starting and reference complexes

Starting complexes for bis(β-diketonato)di(aqua)chromium(III) complexes. β-diketone (2 mmol) was added to a solution of 1 mmol of $Cr(NO_3)_3 \cdot 9H_2O$ in 50 mL of EtOH with stirring at room temperature. After the mixture was dissolved completely in EtOH, 2 mmol of NaOEt was added to this solution. After 3 days stirring, the reaction solution was evaporated under reduced pressure. The crude product was obtained by the addition of dichloromethane and the precipitate was filtered off. The solid was dissolved in 5 mL of EtOH. This solution was loaded on a cation exchange column [SP-TOYOPEARL 550 (Na^+) resin]. The adsorbed band was eluted with 0.1 mol dm^{-3} $NaBF_4$ ethanol solution. Only one band was eluted, which was supposed to be a unipositive ion, leaving highly charged cation complexes on the top of the column. This eluate was evaporated to dryness. After the residue was desalted by extraction with dichloromethane, a powder was obtained. Such powders were characterized as [Cr(β-diketonato)$_2$(H_2O)$_2$]BF_4 by elemental analysis and were used as the starting complexes without further characterization.

Reference complex. [Cr(acac)$_2$(en)]PF_6 was synthesized according to the literature method.[16]

Syntheses of NIT2py complexes

(1) [Cr(acac)$_2$(NIT2py)]PF_6 1. [Cr(acac)$_2$(NIT2py)]PF_6 was synthesized by a modification of the previously reported method.[11a] Yield 75%. Found: C, 42.0; H, 4.97; N, 6.58. $C_{22}H_{30}CrF_6N_3O_6P$ requires C, 42.0; H, 4.80; N, 6.68%.

(2) [Cr(dbm)$_2$(NIT2py)]PF_6 2. NIT2py (1 mmol) was added to a solution of 1 mmol of [Cr(dbm)$_2$(H_2O)$_2$]BF_4 in 50 mL of CH_3CN with stirring in an ice–methanol bath at −15 °C. After 12 h stirring, the solution was evaporated under reduced pressure. The residue was dissolved in 50 mL of EtOH, and 1 mmol of $NaPF_6$ was added to this solution. After 1 day stirring, the solution was evaporated under reduced pressure. The crude product was obtained by adding dichloromethane. The residue was dissolved in 10 mL of $CHCl_3$. This solution was loaded on a HPLC column (LC-908, Japan Analytical Industry Co. Ltd.) and eluted with $CHCl_3$. The first band eluted with $CHCl_3$ contained the desired cation [Cr(dbm)$_2$(NIT2py)]$^+$. After the eluate was condensed, crystallization was carried out by vapor diffusion from dichloromethane–diethyl ether. This complex was recrystallized as violet–green needle-like crystals. Yield 80%. Found: C, 57.2; H, 4.28; N, 4.82. $C_{42}H_{38}CrF_6N_3O_6P$ requires C, 57.5; H, 4.36; N, 4.79%.

The other β-diketonato complexes [Cr(β-diketonato)$_2$(NIT2-py)]PF_6 [β-diketonato = bzac (**3**), acaMe (**4**), acaEt (**5**), aca^{n}Bu (**6**), acaPh (**7**), dpm (**8**), Mehp (**9**)] were obtained by a similar method to that for the dbm complex. Most were obtained as powdery solids except the crystalline acac, dbm and dpm complexes. **3**: 60%. Found: C, 50.2; H, 4.44; N, 5.38.$C_{32}H_{34}CrF_6N_3O_6P$ requires C, 51.0; H, 4.55; N, 5.58%. **4**: 65%. Found: C, 43.8; H, 5.16; N, 6.33. $C_{24}H_{34}CrF_6N_3O_6P$ requires C, 43.8; H, 5.21; N, 6.39%. **5**: 60%. Found: C, 45.0; H, 5.61; N, 6.27. $C_{26}H_{38}CrF_6N_3O_6P$ requires C, 45.6; H, 5.59; N, 6.13%. **6**: 60%. Found: C, 48.2; H, 6.14; N, 5.64. $C_{30}H_{48}CrF_6N_3O_6P$ requires C, 48.5; H, 6.50; N, 5.64%. **7**: 60%, Found: C, 51.7; H, 4.94; N, 5.35. $C_{34}H_{38}CrF_6N_3O_6P$ requires C, 52.2; H, 4.90; N, 5.38%. **8**: 75%. Found: C, 51.0; H, 6.78; N, 5.47. $C_{34}H_{54}CrF_6N_3O_6P$ requires C, 51.2; H, 6.82; N, 5.27%. **9**: 65%. Found: C, 46.9; H, 5.91; N, 5.81. $C_{28}H_{42}CrF_6N_3O_6P$ requires C, 47.1; H, 5.93; N, 5.89%.

Crystallography

A violet–green square columnar crystal of [Cr(dpm)$_2$(NIT2-py)]PF_6 was sealed in a glass capillary with epoxy resin. X-Ray intensities ($2\theta_{max}$ = 55) were measured at 23 °C with graphite-monochromate Mo-Kα radiation (λ = 0.71069 Å) on an automated Rigaku AFC-7R four-circle diffractometer using the ω–2θ scan technique. There was no serious decomposition. The structure was solved by direct methods using the SHELXS86 program[17] and refined on F^2 with all independent reflections using the SHELXS97 program.[17] All calculations were carried out using a TeXsan[18] software package.

CCDC reference number 164248.

See http://www.rsc.org/suppdata/dt/b1/b104092h/ for crystallographic data in CIF or other electronic format.

Measurements

UV–vis spectra were obtained by a Perkin Elmer Lamda 19 spectrophotometer. Low-temperature UV–vis spectra were measured at 200,100,50 and 10 K using the same spectrophotometer with an Oxford Cryostat DN1704 (static) in a film made from cellulose acetate with acetonitrile. Magnetic susceptibility data were measured at 2000 Oe between 2 and 300 K by using a SQUID susceptometer (MPMS-5S, Quantum Design). Pascal's constants were used to determine the constituent atom diamagnetism values. Resonance Raman spectra were measured in the solid state using a Jasco NR1800 spectrophotometer at room temperature using Ar laser lines (488.00 and 514.50 nm), the He–Ne laser line (632.80 nm), and dye laser lines (584.47 and 606.27 nm) as excitation sources. Luminescence measurement were carried out in the solid state using a Jasco NR1800 spectrophotometer at 5, 50, 120 and 150 K.

Results and discussion

Preparation and characterization

The starting complexes [Cr(β-diketonato)$_2$(H_2O)$_2$]BF_4 for the synthesis of a series of NIT2py complexes could not be prepared by the preparative method in aqueous solution used for the corresponding bis(acac) diaqua complexes.[19] The present method in ethanol solution is generally adopted in the preparation of the β-diketonato diaqua complexes. The diaqua complexes were obtained as an equilibrium mixture of *cis* and *trans* geometrical isomers, but no separation was attempted. The synthetic method of the new [Cr(β-diketonato)$_2$(NIT2py)]PF_6 complexes was different from that of [Cr(acac)$_2$(NIT2py)]PF_6.[12] When [Cr(β-diketonato)$_2$(H_2O)$_2$]BF_4 and NIT2py were mixed in acetonitrile, [Cr(β-diketonato)$_2$(NIT2py)]PF_6 complexes were found to form in solution at room temperature. However, during the formation reaction at room temperature, NIT2py was changed to IM2py. The most remarkable case was seen for the hexafluoroacetylacetonato (hfac) complex. It was confirmed from UV–vis spectra in acetonitrile that NIT2py in [Cr(hfac)$_2$(NIT2py)]$^+$ is deoxygenated to IM2py in [Cr(hfac)$_2$(IM2py)]$^+$ in 1 day at room temperature. The deoxygenation reaction rates were found to depend on the nature of the β-diketonate. Deceleration of the reaction rate by lowering the temperature resulted in the successful isolation of the pure complexes [Cr(β-diketonato)$_2$(NIT2py)]PF_6 except for the hfac complex. Satisfactory elemental analyses for these complexes confirmed the chemical formula with no crystallization solvent, suggesting the chelation of NIT2py.

Molecular structure

Crystallographic data for [Cr(dpm)$_2$(NIT2py)]PF_6 are listed in Table 1. Selected bond lengths, bond angles, torsion angles, and dihedral angles are summarized in Table 2 and the molecular structure is shown in Fig. 1. This is an octahedral complex characterized by chelation of NIT2py through the pyridyl nitrogen and nitronyl nitroxide oxygen leading to a six-membered ring, together with two chelated dpm ligands. The other β-diketonato complexes are expected to have the same structure as the dpm

Table 1 Crystallographic data for $[Cr(dpm)_2(NIT2py)]PF_6$ **8**

Formula	$C_{54}H_{34}CrF_6N_3O_6P$
Formula weight	797.786
T/°C	23
Crystal system	Monoclinic
Space group	$P2_1/a$
a/Å	13.940(4)
b/Å	31.19(1)
c/Å	13.960(4)
β/°	137.03(2)
V/Å^3	4137(2)
Z	4
D_c/g cm^{-3}	1.281
μ(Mo-Kα)/cm^{-1}	0.385
$R1$ [a]	0.070
$wR2$ [b]	0.296

[a] $R1 = \Sigma||F_o| - |F_c||/\Sigma|F_o|$. [b] $wR2 = [\Sigma w(|F_o| - |F_c|)^2/\Sigma w|F_o|^2]^{1/2}$, $w^{-1} = \sigma_c^2(F_o) + (0.00022|F_o|)^2$.

Table 2 Selected bond distances (Å), bond angles (°), torsion angles (°) and dihedral angles (°) for $[Cr(dpm)_2(NIT2py)]PF_6$

Bond distance			
Cr–O(1)	1.962(5)	O(2)–N(2)	1.250(8)
Cr–O(21)	1.929(5)	N(1)–C(1)	1.331(9)
Cr–O(22)	1.947(5)	N(2)–C(3)	1.524(10)
Cr–O(41)	1.932(5)	N(3)–C(8)	1.342(8)
Cr–O(42)	1.936(5)	N(3)–C(12)	1.335(9)
Cr–N(3)	2.091(6)	C(1)–C(8)	1.452(9)
O(1)–N(1)	1.293(7)		
Bond angle			
O(1)–Cr–O(21)	178.6(2)	O(22)–Cr–O(42)	178.4(2)
O(1)–Cr–O(22)	89.1(2)	O(22)–Cr–N(3)	92.9(2)
O(1)–Cr–O(41)	88.0(2)	O(41)–Cr–O(42)	90.3(2)
O(1)–Cr–O(42)	92.4(2)	O(41)–Cr–N(3)	175.5(2)
O(1)–Cr–N(3)	88.1(2)	O(42)–Cr–N(3)	87.7(2)
O(21)–Cr–O(22)	89.7(2)	Cr–O(1)–N(1)	122.5(4)
O(21)–Cr–O(41)	91.2(2)	O(1)–N(1)–C(1)	126.6(5)
O(21)–Cr–O(42)	88.8(2)	O(2)–N(2)–C(1)	128.5(7)
O(21)–Cr–N(3)	92.8(2)	Cr–N(3)–C(8)	126.1(5)
O(22)–Cr–O(41)	89.3(2)	Cr–N(3)–C(12)	116.6(5)
Torsion angle			
N(1)–C(1)–C(8)–N(3)	−17.5(11)		
Dihedral angle			
Plane 1 [a]–plane 2 [b]	18.59	Plane 1–plane 4 [d]	146.89
Plane 1–plane 3 [c]	31.02	Plane 2–plane 3	20.94

[a] Plane 1: O(1), N(1), C(1), N(2), O(2). [b] Plane 2: N(3), C(8), C(9), C(10), C(11), C(12). [c] Plane 3: Cr, O(1), N(3). [d] Plane 4: Cr, O(1), N(1).

complex in view of the similarity of their UV–vis spectral and SQUID magnetic susceptibility as described below.

The two N–O lengths of the nitronyl nitoxide moiety are similar to those of other NIT2py complexes.[9–11a] This fact suggests the existence of the nitronyl nitroxide radical in the complex. The coordinated O(1)–N(1) length [1.293(7) Å] for the NIT2py is longer than the uncoordinated O(2)–N(2) length [1.250(8) Å] as observed for other metal NIT2py complexes [*e.g.*, NIT2py Ni(II) complex [11a]). The Cr–O bond lengths for the dpm ligands are in the range 1.93–1.95 Å, which are shorter than those (1.94–1.98 Å) of the corresponding $[Cr_2(dpm)_4(\mu\text{-}MeO)_2]$ complexes.[20] As shown in Table 2, the bite angle 88.1(2)° for O(1)–Cr–N(3) is larger compared with those of [Ni(β-diketonato)(tmen)(NIT2py)]PF_6 [11a] and $[Ni(hfac)_2(NIT2py)]$.[9] The dihedral angles around the NIT2py moiety together with the torsion angle of N(1)–C(1)–C(8)–N(3) for the NIT2py are smaller than those of [Ni(β-diketonato)(tmen)(NIT2py)]PF_6 [11a] and $[Ni(hfac)_2(NIT2py)]$.[9] This indicates that the NIT2py chelate in the Cr(III) complex is more flattened than those of the Ni(II) complexes. Judging from the sign of the torsion angle of N(1)–C(1)–C(8)–N(3) for the NIT2py, this complex has a Δ

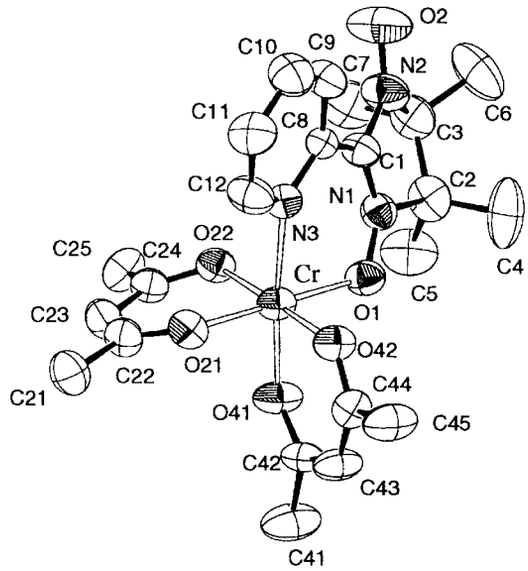

Fig. 1 View of the molecular structure of $[Cr(dpm)_2(NIT2py)]PF_6$ **8**. ^{t}Bu groups have been omitted for the sake of clarity.

absolute configuration (Fig. 1) with the three chelates around a Cr(III) ion adopting a λ(lel) conformation of NIT2py and *vice versa*, in terms of the IUPAC definition, as found in the Ni(II) complexes.[11a] There seems to be no intermolecular interactions in view of the crystal packing around the complex.

Magnetic properties

The product of the molar magnetic susceptibility (χ_M) and temperature (T) $\chi_M T$ *vs.* T plot for $[Cr(acac)_2(NIT2py)]PF_6$ is shown in Fig. 2. The $\chi_M T$ values are smaller at room temperature than the calculated value for an uncorrelated system containing a chromium(III) cation and NIT2py radical (S=3/2 + 1/2) ($\chi_M T$ = 2.25 emu K mol^{-1}) and decrease with lowering the temperature, suggesting an antiferromagnetic interaction [4a] between Cr(III) and the NIT2py radical. $\chi_M T$ *vs.* T plots for other $[Cr(\beta\text{-diketonato})_2(NIT2py)]PF_6$ complexes show a similar pattern. The magnetic coupling constants J_{obs} involving a chromium(III) ion and NIT2py were estimated by fitting the magnetic susceptibilities to a two-spin system (S_1 = 3/2, S_2 = 1/2).[21] The J_{obs} values thus obtained with R values equal to 10^{-3}–10^{-4} are summarized together with the g values in Table 3. The J_{obs} values range from −9.05 to −98.6 cm^{-1}; $[Cr(acaX)_2(NIT2py)]PF_6$ type complexes with 3-substituted acac ligands

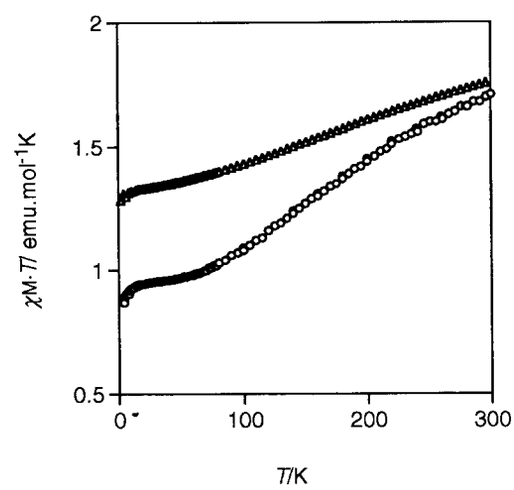

Fig. 2 Temperature dependence of the magnetic susceptibilities for $[Cr(acac)_2(NIT2py)]PF_6$ **1** (○) and $[Cr(acaMe)_2(NIT2py)]PF_6$ **4** (Δ) in the form of $\chi_M T$ *vs.* T.

Table 3 Magnetic and optical data for the NIT2py Cr(III) complexes

Compound	J_{obs} $(g)^a$	$\varepsilon_{SF}{}^b$	$\varepsilon_{CT}{}^c$	$E_{CT}{}^d$	$E_{CT}{}^e$	$(\varepsilon_{SF}/\varepsilon_{CT})(E_{CT})^2/(E_{CT})^f$
1 $[Cr(acac)_2(NIT2py)]PF_6$	−61.6 (2.00)	327	641	17.3	4.00	0.472
2 $[Cr(dbm)_2(NIT2py)]PF_6$	−70.0 (2.00)	325	648	17.3	4.05	0.475
3 $[Cr(bzac)_2(NIT2py)]PF_6$	−30.2 (2.01)	285	589	17.3	4.00	0.447
4 $[Cr(acaMe)_2(NIT2py)]PF_6$	−9.05 (2.06)	230	504	17.1	4.01	0.429
5 $[Cr(acaEt)_2(NIT2py)]PF_6$	−36.5 (2.02)	265	536	17.2	4.07	0.477
6 $[Cr(aca^nBu)_2(NIT2py)]PF_6$	−12.3 (2.01)	279	567	17.1	4.01	0.462
7 $[Cr(acaPh)_2(NIT2py)]PF_6$	−19.4 (2.02)	234	479	17.2	4.03	0.460
8 $[Cr(dpm)_2(NIT2py)]PF_6$	−98.6 (2.00)	346	631	17.3	3.97	0.500
9 $[Cr(Mehp)_2(NIT2py)]PF_6$	−49.0 (2.00)	337	660	17.3	4.02	0.478

[a] Observed J values/cm^{-1}. [b] Molar absorption coefficient for the spin-forbidden transition/mol^{-1} dm^3 cm^{-1}. [c] Molar absorption coefficient for the MLCT transition/mol^{-1} dm^3 cm^{-1}. [d] MLCT transition energy/$10^3 cm^{-1}$. [e] The energy difference between the spin-forbidden and MLCT transition/10^3 cm^{-1}. [f] $J_{AF}/10^3$ cm^{-1}.

tend to give small J_{obs} values in the range from −9.05 to −36.5 cm^{-1}. These J_{obsd} values of $[Cr(\beta\text{-diketonato})_2(NIT2py)]PF_6$ exhibit no relationship with the Hammett constants unlike the corresponding Ni(II) complexes,[11a] but are fairly well related to the acid dissociation constants K_a of the β-diketones; J_{obsd} values increasing with increasing K_a.

UV absorption spectra

UV spectra of $[Cr(acac)_2(NIT2py)]PF_6$ are compared with those of NIT2py and the nonradical ethylenediamine (en) complex $[Cr(acac)_2(en)]PF_6$ as shown in Fig. 3. The absorption

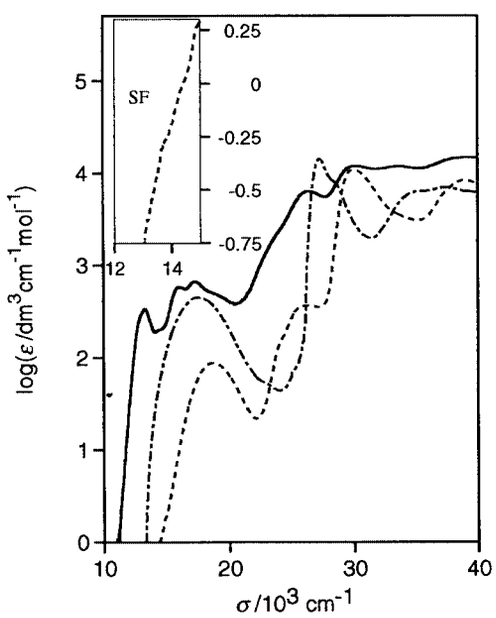

Fig. 3 Absorption spectra of $[Cr(acac)_2(NIT2py)]PF_6$ **1** (——), $[Cr(acac)_2(en)]PF_6$ (– – –) and NIT2py (– · – · –) in CH_3CN at room temperature. Inset: enlarged absorption curve with a logarithmic ordinate for $[Cr(acac)_2(en)]PF_6$ (– – –) in CH_3CN at room temperature.

bands of NIT2py at 17.8×10^3 cm^{-1} and 27.4×10^3 cm^{-1} are due to intraligand n–π* and π–π* transitions, respectively.[22] The absorption bands around 27×10^3 cm^{-1} of $[Cr(\beta\text{-diketonato})_2(NIT2py)]^+$ correspond to the π–π* transitions of NIT2py in view of the similarity in position and intensity with the β-diketonato (acac, Mehp, dpm) complexes. However, the absorption intensities of $[Cr(dbm \text{ or } bzac \text{ and } acaX)_2(NIT2py)]^+$ are larger than those for the other β-diketonato complexes, owing to the overlap with the phenyl π–π* transition in the dbm or bzac ligands with the π–π* transition or charge transfer transition originating from the other acaX ligands. Since the higher frequency absorption band of $[Cr(acac)_2(NIT2py)]^+$ at 30.0×10^3 cm^{-1} is analogous in position and intensity to that of $[Cr(acac)_2(en)]^+$ at 30.0×10^3 cm^{-1}, this is assigned to a π–π* transition or charge transfer originating from the acetylacetonato ligand. Similarly to the Ni(II) complexes,[11a] the additive character of the non-radical bis(β-diketonato) Cr(III) complexes and NIT2py is also seen for the electronic transitions in the ultraviolet region of the NIT2py Cr(III) complexes, and they are not necessarily affected by NIT2py coordination.

Visible absorption spectra: charge-transfer transitions

In the visible region where the n–π* intraligand band of NIT2py or the first spin-allowed d–d $^4A_2 \longrightarrow {}^4T_2$ band for the non-radical Cr(III) complexes are observed, the characteristics of the absorption spectra of $[Cr(\beta\text{-diketonato})_2(NIT2py)]^+$ at $16.0–17.0 \times 10^3$ cm^{-1} are different from those of NIT2py and the non-radical Cr(III) complex as shown in Fig. 3. The band intensities are much larger than those of the latter compounds and the band envelope has vibronic structure; two components were observed with a spacing of about 2000 cm^{-1} as peaks or shoulders. The molar absorption coefficients (ε) of each component in this region was found to be influenced by the nature of the β-diketonato coligands as seen in Fig. 4. From these spec-

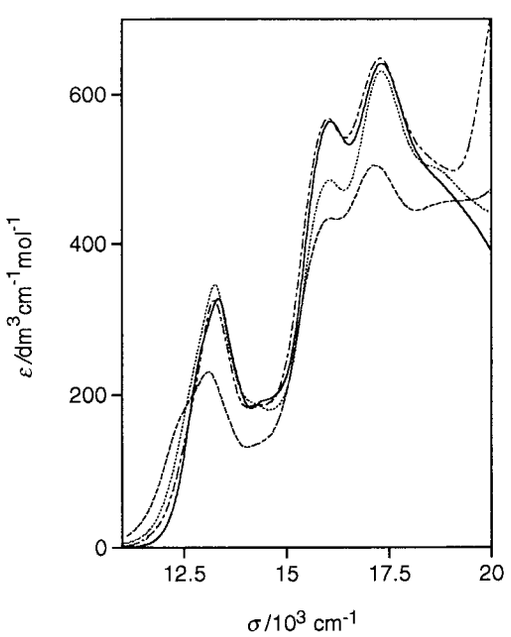

Fig. 4 Absorption spectra of complex **1** (——), **2** (– · – · –), **4** (– – –) and **8** (· · · · ·) in CH_3CN at room temperature.

tral observations, the visible absorption bands are assigned not to intraligand nor d–d transitions, but rather to charge transfer (CT) transitions as verified by resonance Raman spectra (*vide infra*).

The resonance Raman spectra of $[Cr(acac)_2(NIT2py)]PF_6$ in the solid state are shown for a variaty of excitation wavelengths

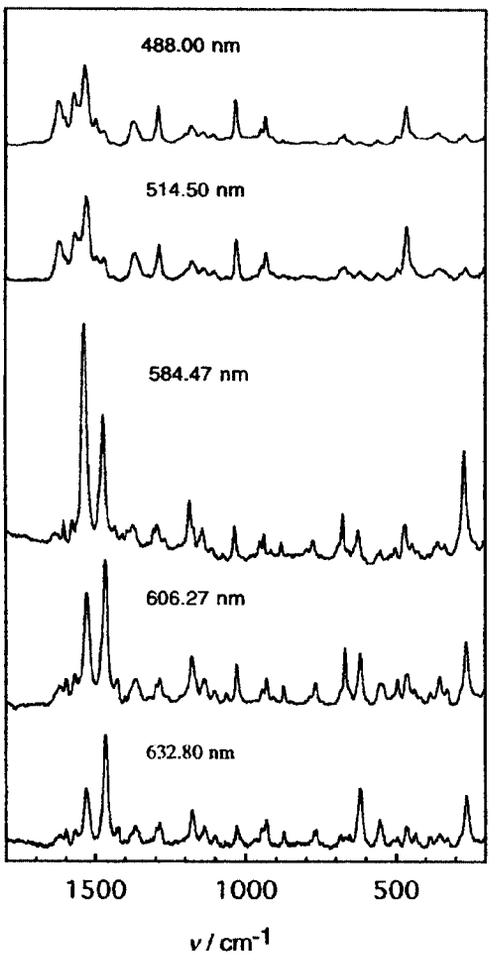

Fig. 5 Resonance Raman spectra of $[Cr(acac)_2(NIT2py)]PF_6$ **1** recorded using 488.00, 514.50, 584.47, 606.27 and 632.80 nm laser lines.

in Fig. 5. In Raman spectra in resonance with the components in the region (16.0–18.0) × 10^3 cm^{-1}, significant intensity enhancement was observed, especially for the bands around 1530 and 1468 cm^{-1} which can be assigned to the stretching vibrations of the O–N=C moiety of the NIT2py ligand. The remaining enhanced peak at 614 cm^{-1} may be due to the Cr–O,N stretching. Thus, as seen from the excitation profile in Fig. 6, the (16–18) × 10^3 cm^{-1} components are assignable to charge transfer transitions. The intensity enhancement of this band on lowering the temperature (Fig. 7) substantiates an assignment (Fig. 8) to the triplet–triplet metal t_{2g} ⟶ ligand SOMO π* (ML(CT) transition. This is also supported by the blue shift in more polar solvents (from CH_2Cl_2 and CH_3CN to CH_3OH).

Near-infrared absorption spectra: spin-forbidden d–d transitions

For the radical complexes $[Cr(\beta\text{-diketonato})_2(NIT2py)]^+$, the absorption peaks around 13.3 × 10^3 cm^{-1} were intensified by several hundreds times compared with those of the non-radical complex $[Cr(acac)_2(en)]^+$ in the corresponding region as shown in Fig. 3. As shown in Fig. 2 of our previous communication,[12] the MCD sign in this region is similar to that of $[Cr(acac)_2(en)]^+$, though their intensities were different from each other along with small peak shifts. The CD peaks of the en complex were observed in the same region as the near infrared band of the NIT complexes.[23] These facts suggest that they originate from spin forbidden $^4A \longrightarrow {}^2E,{}^2T$ d–d transitions. Such enormous intensity enhancements in the spin-forbidden transition are ascribed to exchange coupling between the Cr^{3+} and the NIT2py radical. However, the extent of the enhancement is much smaller as compared with the strong coupling case for the semiquinone complexes.[5] Such less enhanced intensities are inferred from the moderate magnetic couplings, but are little

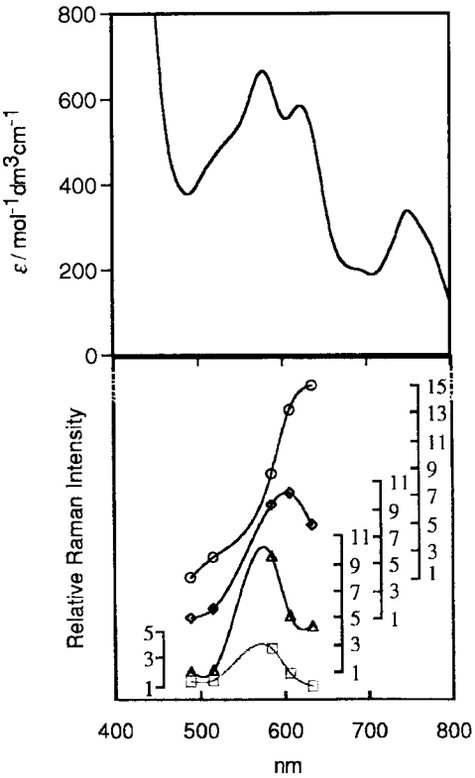

Fig. 6 Excitation profiles (bottom) with visible spectra (top) of $[Cr(acac)_2(NIT2py)]PF_6$ **1**; 1530cm^{-1} (□); 1468cm^{-1} (◇); 614cm^{-1} (○); 258cm^{-1} (△).

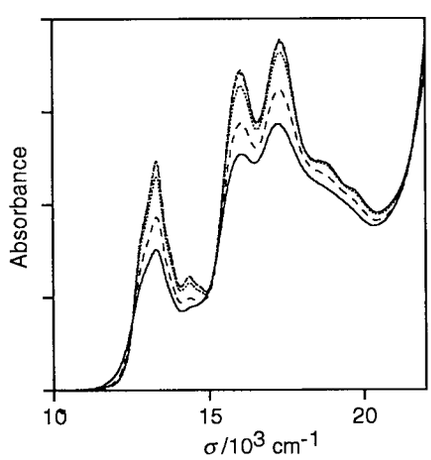

Fig. 7 Absorption spectra of complex **1** in an acetate cellulose film at 30 K (——), 200 K (– – –), 100 K (· · · · · ·), 50 K (— · — · —) and 10 K (------).

varied with the J_{obs} values in contrast to the case of the Ni (II) complexes.[11a]

The exchange coupled ground quartet state consists of the triplet $^3L_0$ ($^4A_2$) and quintet $^5L_0$ ($^4A_2$) states, whereas the excited doublet state $^2\Gamma$ (Γ = E and/or T_1) generates the triplet ^3L_D ($^2\Gamma$) and singlet ^1L_D ($^2\Gamma$) states as shown in Fig. 8. Therefore, the quartet–doublet spin-forbidden d–d transitions of $[Cr(\beta\text{-diketonato})_2(NIT2py)]^+$ become formally spin-forbidden or substantially spin-allowed between the exchange coupled triplets as a result of the breakdown of $\Delta S = 0$ restriction. This assignment is supported by the absorption band intensity enhancement with lowering the temperature (Fig. 7), which result from the Boltzmann population of the triplet level in the ground state, in accordance with the antiferromagnetic interaction observed by the magnetic susceptibility measurements. The difference between the magnetic and spectroscopic properties for the NIT2py Cr(III) complexes with various β-diketonates

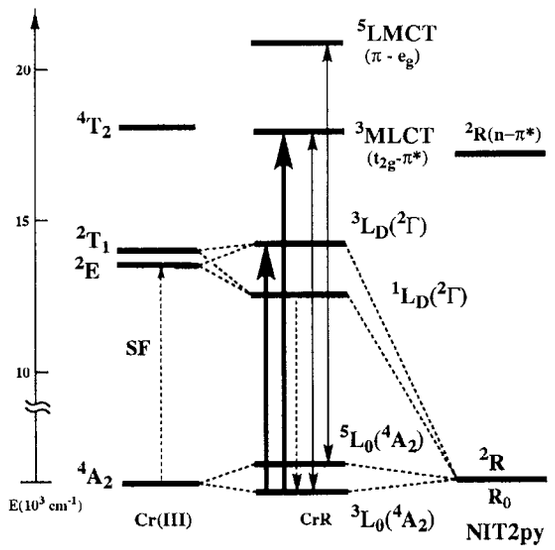

Fig. 8 Energy levels of the spin-allowed and spin-forbidden d–d transitions. (⟶) absorption spectra; (·····) spin-forbidden absorption and emission; (⟵⟶) configurational interactions between the ground and CT states with the same spin multiplicity.

are examined in terms of the exchange mechanism for the intensity enhancement in the formally spin-forbidden d–d transition region as discussed below.

Luminescence spectra

The remeasurement of the luminescence spectra of [Cr(acac)$_2$(NIT2py)]PF$_6$ **1** demonstrated similar behavior except for the peak position to the previously reported value.[12] The observed peak at 11 350 cm^{-1} is located at a lower frequency than the lowest frequency absorption peak corresponding to the spin-forbidden [$^3L_0$ ($^4A_2$) ⟶ ^3L_D ($^2\Gamma$)] triplet–triplet transition around 13300 cm^{-1} as shown in Fig. 9. This shows a large

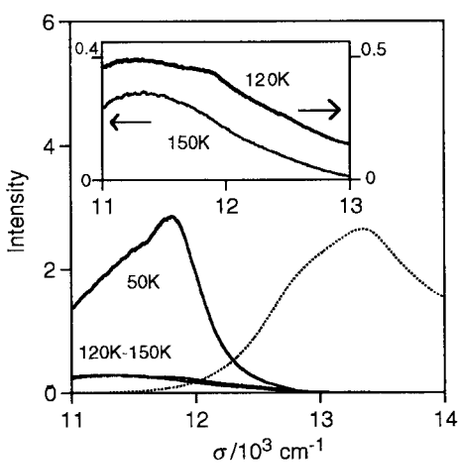

Fig. 9 Luminescence (solid lines) in the solid at 150, 120 and 50 K and absorption spectra (dotted line) in CH_3CN at room temperature of [Cr(acac)$_2$(NIT2py)]PF$_6$ **1**. Inset: enlarged spectra at 120 and 150 K.

Stokes shift involving the ^1L_D ($^2\Gamma$) ⟶ $^3L_0$ ($^4A_2$) emission, for which the corresponding absorption bands should be too weak to observe owing to the definitely spin-forbidden triplet–singlet transitions (Fig. 8). Thus, antiferromagnetic coupling is suggested between the lowest excited doublet state of the Cr(III) moiety and the ground doublet state of the NIT2py radical. On cooling to 120 K, another luminescence peak appears at a higher frequency of *ca.* 11 800 cm^{-1} other than the main 11350 cm^{-1} peak at 150 K. Further cooling to 50 K leads to the 11 800 cm^{-1} peak becoming more intense by about ten times than that at 120 K, and the lower frequency 11 350 cm^{-1} peak becomes invisible, as shown in Fig. 9. This variable temperature behavior suggests intensity variation of two peaks on cooling but no blue shift. A similar intensification of the higher frequency peak around 11 800 cm^{-1} on cooling is seen for the other [Cr(β-diketonato)$_2$(NIT2py)]$^+$ complexes. Apart from the recent claim that the NIR luminescence in Ln(III) complexes with two chelating NITBzImH radicals arises from ligand-centered transitions,[24] the suggestion that the present anomalous temperature variable luminescence originates from the ligand field d–d transitions in view of the peak position is the only other reported instance.

The origin of the intensification of the spin-forbidden transitions

Though the formally spin-forbidden $^2L_0$ ($^3A_2$) ⟶ ^2L_s (^1E) transitions of the NIT2py Ni(II) complexes with various types of β-diketonates show a large range of absorption intensities [120–480 mol^{-1} dm^3 cm^{-1} for the molar absorption coefficients ε_{max}(SF)],[11a] the corresponding Cr(III) complexes show only a small range of $^3L_0$ ($^4A_2$) ⟶ ^3L_D ($^2\Gamma$) transition intensities [ε_{max}(SF) = 234–346 mol^{-1} dm^3 cm^{-1}] as shown in Table 3. The range of the MLCT band intensity [ε_{max} = (CT) = 479.0–630.9 mol^{-1} dm^3 cm^{-1}) for the Cr(III) complexes is also much smaller than that of ε_{max} (CT) for the Ni(II) complexes. In addition ε_{max}(SF) is found to increase with increasing ε_{max} (CT) as shown in Table 3. These facts strongly suggest a connection among the ε_{max} (CT), ε_{max}(SF) and J_{obs} values in multi-spin coupled systems; in other words, the formally spin-forbidden $^3L_0$ ($^4A_2$) ⟶ ^3L_D ($^2\Gamma$) transition can attain the integrated intensity I_{SF} by borrowing the t_{2g}–π* SOMO charge transfer integrated intensity I_{CT} through an exchange mechanism.[25]

According to the exchange mechanism, the spin-forbidden $^3L_0$ ($^4A_2$) ⟶ ^3L_D ($^2\Gamma$) transition of Cr(III) radical complexes is made allowed by mixing of the MLCT excited states through perturbation, *i.e.*, *via* modification of the electron transfer integral between the Cr (t_{2g}) and NIT2py (SOMO π*). The real triplet (doublet) wave function is given by eqn (1).

$$\Psi(^3\phi(^2\Gamma)) = \Psi_0(^3\phi(^2\Gamma)) + b\Phi(^3\phi(\mathrm{MLCT})) \qquad (1)$$

This contains an admixture of the triplet MLCT wave function, where $\Psi_0(^3\phi^2(\Gamma))$ and $\Phi(^3\phi\mathrm{MLCT}))$ are approximated to represent $|t_{2g}{}^+t_{2g}{}^+t_{2g}{}^-\pi^{*+}|$ and $|t_{2g}{}^+t_{2g}{}^+\pi^{*-}\pi^{*+}|$.

Spin-forbidden transitions attain a transition intensity or integrated intensity I_{SF}, by acquiring a small part,

$$b = <|t_{2g}{}^+t_{2g}{}^+t_{2g}{}^-\pi^{*+}|h|t_{2g}{}^+t_{2g}{}^+\pi^{*-}\pi^{*+}|>/\Delta E_{CT}$$
$$= <|t_{2g}{}^-|h|\pi^{*-}|>/\Delta E_{CT} = h(\mathrm{CT})/\Delta E_{CT}$$

of that of the spin-allowed MLCT where ΔE_{CT} is the difference ($E_{CT} - E_{SF}$) between the transition energies, E_{CT} and E_{SF}, from the triplet ground state to the ^{3}MLCT and the ^3L_D ($^2\Gamma$), respectively, as given by eqn. (2).

$$I_{SF} = b^2 I_{CT} = (h(\mathrm{CT})/\Delta E_{CT})^2 I_{CT} \qquad (2)$$

According to the experimental correlation between ε_{max}(SF) and ε_{max}(CT) (*vide supra*), the term h(CT)/ΔE_{CT} in eqn. (2) is constant with variation of the coligands.

Spin-forbidden band intensity and magnetic interaction

The configurational interaction with the triplet MLCT excited state results in stabilizing the triplet ground state level by $h(\mathrm{CT})^2/E_{CT}$ (Fig. 8). Thus, the exchange coupling constant J_{AF} [eqn. (4)] is expressed in terms of the spin-forbidden and MLCT transition intensities ratios from eqns. (2) and (3) with

$$J_{AF} = h(\mathrm{CT})^2/E_{CT} \qquad (3)$$

neglect of the exchange integral K or by considering the antiferromagnetic interaction through the charge (electron) transfer integral h(CT).[26]

$$J_{AF} = (I_{SF}/I_{CT})(\Delta E_{CT})^2 \propto \{\varepsilon_{max}(SF)/\varepsilon_{max}(CT)\}(\Delta E_{CT})^2/E_{CT} \quad (4)$$

As in eqn. (4),[27] the integrated intensity I_{SF} may be approximated by the product of the molar absorption coefficient(ε_{max}) and the half-bandwidth ($\Delta_{1/2}$). Actually, since $\Delta_{1/2}$ of the MLCT components are similar to those of the formally spin-forbidden bands, the ratios of $\varepsilon_{SF}/\varepsilon_{CT}$ are taken for simplicity instead of I_{SF}/I_{CT} in the following discussion. The ratios of $\varepsilon_{SF}/\varepsilon_{CT}$ are almost constant as seen above, and the MLCT transition energy E_{CT} and the energy difference between the MLCT and the spin-forbidden transition energy ΔE_{CT} do not change with different β-diketonates. This indicates that the value of

$$J_{AF} \propto \{\varepsilon_{max}(SF)/\varepsilon_{max}(CT)\}(\Delta E_{CT})^2/E_{CT}$$

is almost constant for different β-diketonates, though the J_{obs} values vary considerably from *ca.* −9 to −99 cm^{-1} (Table 3). That is, the antiferromagnetic interaction is not affected by the coligands [eqn. (5)].

$$J_{obs} = J_{AF} + J_F \quad (5)$$

Since the J_{obs} values consist of the antiferromagnetic and ferromagnetic contribution ($J_{AF} + J_F$) as in eqn. (5), the variation of the J_{obs} values is associated with that of the J_F values. In other words, the coligand effect is operative in the ferromagnetic interaction, but not in the antiferromagnetic one. Therefore, the magnetic interactions of the bis(β-diketonato)Cr(III) complexes mainly vary with the change of the ferromagnetic coupling of the second term (J_F) of eqn. (5), in contrast to the case of NIT2py Ni(II) complexes where variation of the J_{obs} values is governed through the antiferromagnetic coupling of the first term (J_{AF}). The reverse role in the coligand effect on the J_{obs} values may be ascribed to the difference in the respective magnetic orbitals [$t_{2g}(d_\pi)$ for Cr(III) and $e_g(d_\sigma)$ for Ni(II)]. This point will be discussed in more detail in connection with the magneto-optical properties for two series of Ni(II) and Cr(III) IM2-py complexes.[28]

Conclusions

The present spectroscopic studies along with the magnetic properties can elucidate in some detail the spectral behavior in terms of position and intensity of the ligand field ^2E and $^2T_1$ states of the Cr(III) complexes which are coupled with the NIT2py radical ligand. The J_{obs} values are found to vary with the J_F values, but we are not yet in a position to obtain a correlation between them through the coligand effect. Although our initial attempts to obtain any correlation between the magnetic and the spectroscopic properties through the coligand effect are as yet unsuccessful, the hypothesis of variable J_F values with varying coligands may be rationalized by considering the lowest LMCT which generates only a quintet but not a triplet according to the formulation for the ferromagnetic interaction in superexchange for dinuclear metal complexes.[29] The quintet LMCT is a $\pi \longrightarrow e_g$ transition to the quintet excited state $|t_{2g}^{+}t_{2g}^{+}t_{2g}^{+}e_g^{+}\pi^{-}\pi^{*}+|$ from the quintet ground state $|t_{2g}^{+}t_{2g}^{+}t_{2g}^{+}\pi^{-}\pi^{+}\pi^{*+}|$. The stabilization of the quintet level in the ground state or the variation of J_F values could result from a difference in the configurational interaction ($<|e_g^{+}|h|\pi^{+}|>$) between the quintet ground and excited states. Our future goal will be to explore more detailed or quantitative correlations between J_F and the electronic properties of the coligands as inferred from the relation between J_{obs} or J_F and the acid dissociation constants of the β-diketones. Another aim is to pursue quantitative complementarity between optical and magnetic properties; elucidating the disagreement between the magnetic interaction derived from the magnetic susceptibility measurements and that estimated from the variable temperature absorption band intensity changes.

Acknowledgements

We gratefully acknowledge support of this research by a Grant-in-Aid for Scientific Research (A)(2) (No.10304056) from the Ministry of Education, Science and Culture.

References

1 H. U. Güdel, in *Magnetic–Structural Correlations in Exchange Coupled Systems*, ed. R. D. Willet, D. Gatteschi, O. Kahn, Reidel, Dordrecht, The Netherlands, 1985, p. 297.
2 P. U. McCarthy and H. U. Güdel, *Coord. Chem. Rev.*, 1988, **88**, 69.
3 (*a*) C. Bellitto and P. Day, *J. Chem. Soc., Dalton Trans.*, 1978, 1207; (*b*) C. Bellitto and P. Day, *J. Chem. Soc., Dalton Trans.*, 1986, 847; (*c*) C. Bellitto and P. Day, *J. Mater. Chem.*, 1992, **2**, 265.
4 (*a*) C. Mathonieres, O. Kahn, J. C. Daran, H. Hilbig and F. H. Kohler, *Inorg. Chem.*, 1993, **32**, 4057; (*b*) C. Mathonieres and O. Kahn, *Inorg. Chem.*, 1994, **33**, 2103; (*c*) C. Cador, C. Mathonieres and O. Kahn, *Inorg. Chem.*, 1997, **36**, 1923.
5 C. Benelli, A. Dei, D. Gatteschi, H. U. Güdel and L. Pardi, *Inorg. Chem.*, 1989, **28**, 3089.
6 A. Sokolowski, E. Bothe, E. Bill, T. Weyhermuller and K. Wieghardt, *Chem. Commun*, 1996, 1671.
7 A. Caneschi, D. Gatteschi and P. Rey, *Prog. Inorg. Chem.*, 1991, **39**, 331.
8 I. Dasna, S. Golhen, L. Ouahab, O. Pena, J. Guillevic and M. Fettouhi, *J. Chem. Soc., Dalton Trans.*, 2000, 129.
9 D. Luneau, F. M. Romero, P. Rey, A. Grand, A. Caneschi, D. Gatteschi and J. Langier, *Inorg. Chem.*, 1993, **32**, 5616.
10 D. Luneau, F. M. Romero and R. Ziessel, *Inorg. Chem.*, 1998, **37**, 5078; F. M. Romero, D. Luneau and R. Ziessel, *Chem. Commun.*, 1998, 551.
11 (*a*) T. Yoshida, T. Suzuki, K. Kanamori and S. Kaizaki, *Inorg. Chem.*, 1999, **38**, 1059; (*b*) T. Yoshida and S. Kaizaki, *Inorg. Chem.*, 1999, **38**, 1054.
12 T. Yoshida, K. Kanamori, S. Takamizawa, W. Mori and S. Kaizaki, *Chem. Lett.*, 1997, 603.
13 Y. Yamamoto, T. Suzuki and S. Kaizaki, *J. Chem. Soc., Dalton Trans.*, 2001, 1566.
14 Y. Yamamoto, T. Suzuki and S. Kaizaki, *J. Chem. Soc., Dalton Trans.*, 2001, 2943.
15 J. H. Osiecki and E. F. Ullman, *J. Am. Chem. Soc.*, 1969, **90**, 1078.
16 S. Kaizaki, J. Hidaka and Y. Shimura, *Inorg. Chem.*, 1973, **12**, 135.
17 G. M. Sheldrick, SHELXS-86, Program for Crystal Structure Determination, Univ. of Göttingen, Germany, 1986.
18 TEXSAN, Single Crystal Structure Analysis Software, Version 1.7, Molecular Structure Corporation, The Woodlands, TX, USA, 1995.
19 H. Ogino, Y. Abe and M. Shoji,, *Inorg. Chem.*, 1988, **27**, 986.
20 H. R. Fischer, D. J. Hodgson and E. Pedersen, *Inorg. Chem.*, 1984, **23**, 4755.
21 W. Wojciechowski, *Inorg. Chim. Acta*, 1967, **1**, 324.
22 E. F. Ullman, J. H. Osiecki, P. Rey and R. Sessoli, *J. Am. Chem. Soc.*, 1972, **94**, 7049.
23 S. Kaizaki, J. Hidaka and Y. Shimura, *Inorg. Chem.*, 1973, **12**, 142.
24 C. Lescop, D. Luneau, G. Bussière, M. Triest and C. Reber, *Inorg. Chem.*, 2000, **39**, 3740.
25 J. Ferguson, H. J. Guggenheim and Y. Tanabe, *J. Phys. Soc. Jpn.*, 1966, **21**, 692.
26 O. Kahn, *Molecular Magnetism*, VCH publisher Inc., 1993, ch. 8.
27 Eqn. (3) in our previous paper[11a] was oversimplified on the assumption of $E_{SF} \ll E_{CT}$ as presented in refs. 5 and 25. In the case of the low energy MLCT ($E_{SF} < E_{CT}$), this should be expressed as the present formulation given in eqn. (4). However, this change has no effect on the subsequent discussion in either case of Ni(II) or Cr(III) complexes.
28 Y. Tsukahara, T. Kamatani, A. Iino, T. Suzuki and S. Kaizaki, to be submitted.
29 (*a*) J. Glerup, D. J. Hodgson and E. Pedersen, *Acta, Chem. Scand., Ser. A*, 1983, **37**, 161; (*b*) H. Weihe and U. Güdel, *Inorg. Chem.*, 1997, **36**, 3632; (*c*) H. Weihe, U. Güdel and H. Toftlund, *Inorg. Chem.*, 2000, **39**, 1351.